Strain localization by fracturing and reaction weakening – a mechanism for initiating exhumation of subcontinental mantle beneath rifted margins

M. R. HANDY[1] & H. STÜNITZ[2]

[1] *Geowissenschaften, Freie Universität Berlin, D-12249 Berlin, Germany*
[2] *Geologisch-Paläontologisches Institut, Universität Basel, CH-4056 Basel, Switzerland*

Abstract: Rift-related strain localization in spinel lherzolite from an exhumed passive continental margin in the Southern Alps involved two stages. (1) Critical fracturing coincided with heterogeneous nucleation of plagioclase, olivine, and hornblende aggregates to form discrete, ultrafine-grained (0.5–0.6 μm) shear zones oriented at high angles to the pre-existing foliation in the host rock. The syntectonic replacement of spinel lherzolite by lower pressure, plagioclase–hornblende lherzolite documents extensional exhumation under high temperature (700–900 °C) conditions accompanied by limited fluid infiltration. Deformation involved a combination of dislocation creep (ol) and diffusion-accommodated viscous granular flow (plag, ol, hbl aggregates). (2) Hydrous deformation at lower temperatures (200–400 °C) involved the formation of serpentine–chlorite mylonite and cataclasite along discrete, anastomozing shear zones oriented at low angles to the pre-existing foliation. Both stages involved drastic weakening, particularly once the shear zones coalesced sub-parallel to the extensional shearing plane. The top of the lithospheric mantle was initially strong, but is inferred to have become weaker than both the underlying mantle and the overlying mafic lower crust. The interconnection of such strong-then-weak delamination zones to form trans-lithospheric extensional shear zones accelerated rifting and led to the exhumation of subcontinental mantle during the late stages of continental breakup.

Mantle rocks are exhumed beneath non-coaxial extensional shear zones in rifted continental margins (Lemoine *et al.* 1987; Lister *et al.* 1991) and slow-spreading ocean ridges adjacent to ocean transform faults (Karsons 1991; Tuscholke & Lin 1994). In both settings, deformation is localized at the lithospheric scale, such that extensional strain is transferred from breakaway normal faults bounding asymmetrical rift basins in the upper crust down to mylonitic shear zones in the lower crust and mantle (Wernicke 1985; Lemoine *et al.* 1987). The geometry of these faults within the crust is partly constrained from structural studies of exposed crustal sections (Brodie & Rutter 1987*a*; Handy 1987) and reflection seismological experiments (McGeary & Warner 1985; Reston 1987; Keen *et al.* 1991), but the mechanisms triggering their nucleation and growth at depth, particularly within the mantle, remain enigmatic. The inaccessibility of active mantle shear zones coupled with their poor resolution in reflection seismological profiles obviously limit our ability to use large-scale geometry at depth as a reliable guide to mantle rheology.

Most models of strain localization harbour the assumption that strain localizes either within pre-existing weak lithologies of a compositionally and rheologically stratified lithosphere (e.g. Ranalli & Murphy 1987) or where a weak mechanical phase nucleates within a stronger lithology (e.g. Kirby 1985). In this paper, we term these two types of weakness, respectively, 'inherited weakness' and 'induced weakness'. Although there is consensus that localization results in bulk weakening once weak zones coalesce, some experimental and theoretical studies show that the onset of localization can also involve hardening if deformation is dilatant or involves a dilational component (Hobbs *et al.* 1990). This raises the possibility that large-scale shear zones initiate not in weak layers of the lithosphere, but in strong or preferentially stressed layers where dilational processes like cataclasis and metamorphic phase transformation are favoured.

To date, evidence for this hypothesis is equivocal. Microstructural studies of upper mantle rocks exposed at the surface reveal that most strain in the upper mantle is accommodated by viscous creep mechanisms (Drury *et al.* 1991; Newman *et al.* 1999; Furusho & Kanagawa 1999). Although fracturing has been identified as a potential localization mechanism in upper mantle rocks (Handy 1989; Vissers *et al.* 1997) and brittle precursors of mylonitic shear zones are ubiquitous in crustal rocks (Mitra 1978; Dixon & Williams 1983; FitzGerald & Stünitz 1993; Evans 1991; Wibberley 1999; Wintsch *et al.* 1995), fractures formed at high temperatures just

From: DE MEER, S., DRURY, M. R., DE BRESSER, J. H. P. & PENNOCK, G. M. (eds) 2002. *Deformation Mechanisms, Rheology and Tectonics: Current Status and Future Perspectives*. Geological Society, London, Special Publications, **200**, 387–407. 0305-8719/02/$15 © The Geological Society of London.

prior to and/or during mylonitization are rarely preserved. Most fractures are associated with late mylonitic or post-mylonitic deformation rather than with the onset of mylonitization. Strain localization is therefore usually attributed to progressive dynamic recrystallization, in some cases enhanced by a transition to grain-size-sensitive creep mechanisms like diffusion-accommodated viscous granular flow (Vissers *et al.* 1995; de Bresser *et al.* 2001). The interconnection of such shear zones is believed to weaken the lithosphere during rifting (Handy 1994; Vissers *et al.* 1995), although the extent of this weakening is debatable.

In this paper, we present evidence that extensional shear zones in ultramafic rocks of the former rifted Apulian continental margin (southern Alps) nucleated in the upper mantle as dilatant shear fractures under fluid-deficient conditions. These fractures are shown to have been nuclei for discrete shear zones containing ultrafine-grained aggregates whose syntectonic mineral assemblage documents decompression during extensional exhumation. Based on an analysis of grain size, distribution and shape characteristics, we discuss the probable deformation mechanisms in these aggregates and the implications thereof for strain-dependent changes in the rheology of the lithospheric mantle in non-volcanic, rifted continental margins. In the final section, we integrate these findings with previous work to propose a qualitative mechanical model for distal parts of the rifted Apulian continental margin.

Geological setting

Structures and metamorphism related to Mesozoic, Tethyan rifting are preserved in several circum-Mediterranean mountain belts, where lower continental crustal and upper mantle rocks were exhumed in the footwall of large extensional faults prior to their incorporation within these Tertiary orogens (Drury *et al.* 1991; Vissers *et al.* 1995 and references therein). These pre-orogenic structures are also well preserved and accessible in the Ivrea–Verbano Zone, located in the westernmost part of the Southern Alps (Fig. 1a). The shear zones investigated in this paper transect the Balmuccia ultramafic body, one of several ultramafic bodies within the northwestern margin of the Ivrea–Verbano Zone.

The Ivrea–Verbano Zone is what was originally the deepest part of a fragmented piece of Paleozoic continental crust, the Ivrea crustal section (Fig. 1b). This crust was attenuated first during Early Permian transtensional tectonics, but especially during Early Mesozoic rifting (Handy & Zingg 1991). Shallower to intermediate levels of this rifted continental crust are exposed in adjacent units to the SE (Strona–Ceneri Zone) and NW (Sesia Zone, Fig. 1). Tertiary tectonics, primarily related to transpression along the Insubric Line (Fig. 1), verticalized the Ivrea–Verbano Zone, essentially exposing a cross section of the intermediate to lower continental crust at the surface (Zingg *et al.* 1990; Handy *et al.* 1999 and references therein). In the Ivrea crustal section, this Tertiary deformation was brittle and did not destroy the penetrative pre-Tertiary (Early Mesozoic and earlier) fabrics and mineral assemblages (Schmid *et al.* 1989).

The Balmuccia ultramafic body (Fig. 2) comprises mostly peridotite (spinel lherzolite) with subordinate pyroxenite bands (e.g. Rivalenti *et al.* 1981). It forms the intrusive base of a layered mafic complex (the Mafic Complex, Fig. 1) that itself intruded pre-Variscan mafic rocks and Carboniferous metasediments some 300–320 Ma (age criteria in Handy *et al.* 1999; Vavra *et al.* 1999). The ultramafic rocks therefore intruded at, or just above, the late Variscan (pre-Permian) crust-mantle boundary (Boudier *et al.* 1984), which is constrained by geobarometric studies to have occupied a depth of about 34–44 km at the time of intrusion (Shervais 1979; Rivalenti *et al.* 1981, 1984; Sinigoi *et al.* 1994). Magmatic way-up criteria indicate that the presently vertical magmatic banding in the Balmuccia ultramafic body (Fig. 2) was subhorizontal at the time of intrusion (Rivalenti *et al.* 1975).

The shear zones described below truncate, and therefore clearly post-date the magmatic to high-grade subsolidus structures related to Variscan orogenesis (Figs 3, 4). These latter structures include a subvertical compositional banding defined by cumulate pyroxenite layers (Fig. 4a) and a penetrative schistosity (oriented about 275°/85°, Fig. 2) locally containing a spinel mineral lineation plunging 50°–60° N. This schistosity is defined by pyroxene and spinel

Fig. 1. Geology of the Ivrea–Verbano Zone. (**a**) Map showing ultramafic bodies named after nearby towns (Balmuccia, Baldissero, Finero, Premosello) within the Mafic Complex. Inset map shows location within Alpine chain, western Europe. (**b**) Cross section of the western Central Alps and Southern Alps showing location of the Ivrea crustal section (modified from Schmid & Kissling 2000). Trace of cross section in (**a**) corresponds to section in (**b**) marked by arrow labelled 'Ivrea crustal cross section'.

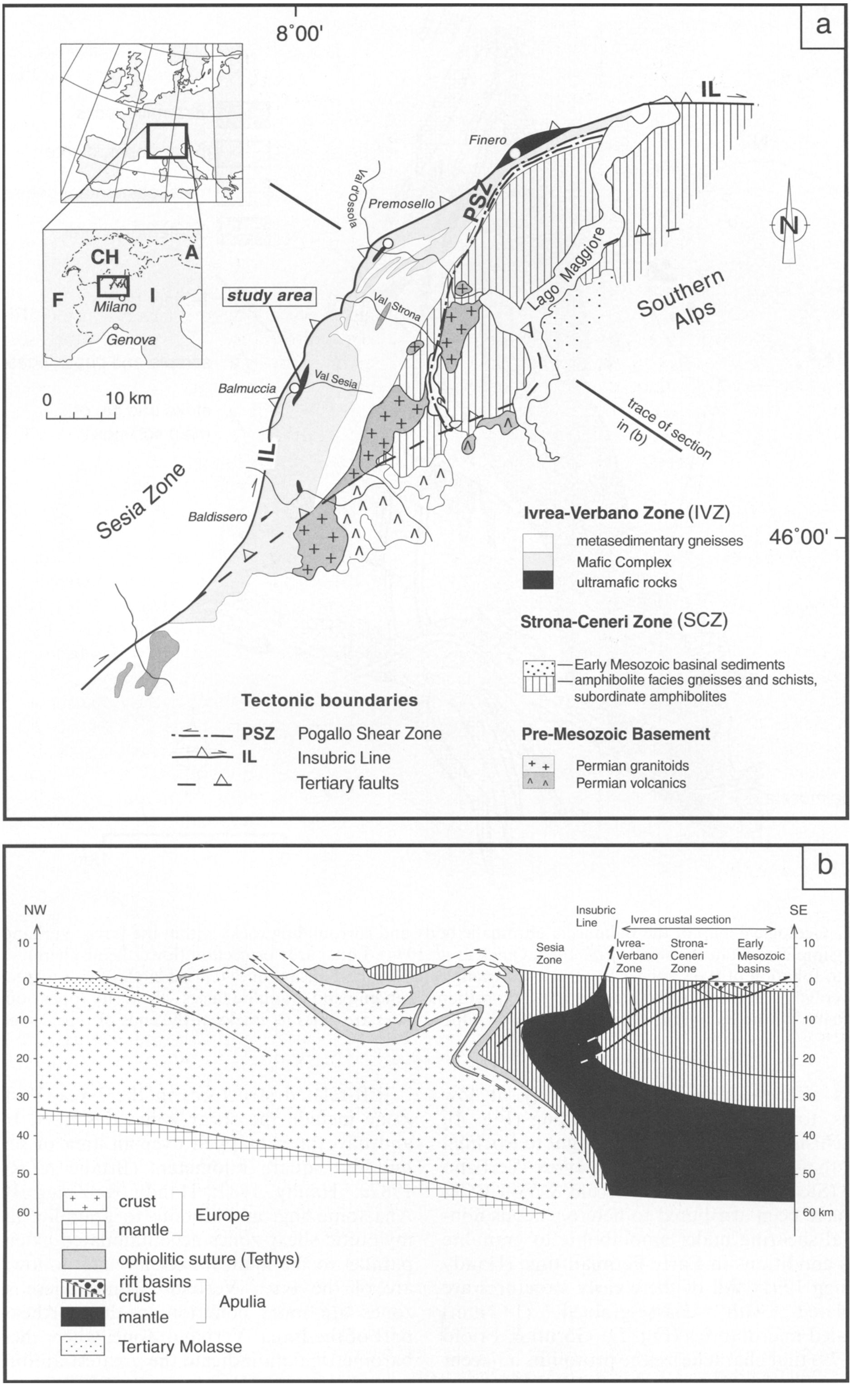
a
8°00'
46°00'
CH
A
F
I
Milano
Genova
0 10 km
study area
Finero
Premosello
Val d'Ossola
PSZ
IL
Lago Maggiore
Southern Alps
N
Val Strona
Val Sesia
Balmuccia
Baldissero
Sesia Zone
trace of section in (b)
Ivrea-Verbano Zone (IVZ)
metasedimentary gneisses
Mafic Complex
ultramafic rocks
Strona-Ceneri Zone (SCZ)
Early Mesozoic basinal sediments
amphibolite facies gneisses and schists, subordinate amphibolites
Pre-Mesozoic Basement
Permian granitoids
Permian volcanics
Tectonic boundaries
PSZ Pogallo Shear Zone
IL Insubric Line
Tertiary faults
b
NW
SE
Insubric Line
Ivrea crustal section
Sesia Zone
Ivrea-Verbano Zone
Strona-Ceneri Zone
Early Mesozoic basins
10
0
10
20
30
40
50
60
60 km
crust
mantle
Europe
ophiolitic suture (Tethys)
rift basins
crust
mantle
Apulia
Tertiary Molasse

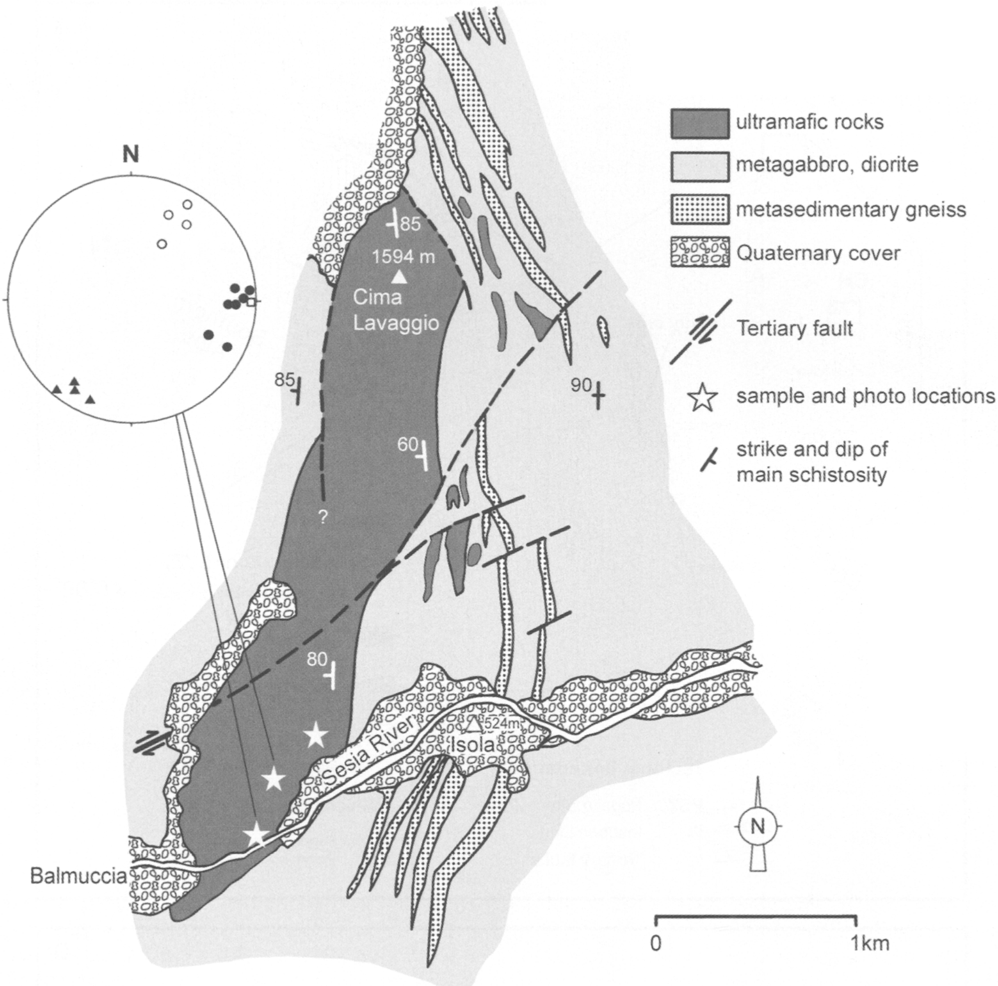

Fig. 2. Geological map of the Balmuccia ultramafic body and surrounding rocks within the Ivrea–Verbano Zone (simplified from Rivalenti *et al.* 1984; Quick *et al.* 1994). Equal area projection (lower hemisphere) with poles to foliation of type 1 shear zones (closed triangles) and type 2 shear zones (closed circles) with respect to the average orientation of the pre-existing compositional banding and granulite facies schistosity (open square) in a quarry of the Balmuccia ultramafic complex. Open circles are poles to cracks at the ends of type 2 shear zones.

grains aligned subparallel, or locally at low angles, to the compositional banding (Fig. 4). The schistosity is axial planar to tight to isoclinal folds that, in other parts of the Ivrea–Verbano Zone (Steck & Tièche 1976; Kruhl & Voll 1978/79), have been attributed to heterogeneous non-coaxial shearing under amphibolite to granulite facies conditions in Early Permian time (Handy & Zingg 1991). All of these early structures are associated with coarse-grained (1–2 mm) annealed microfabrics (Fig. 5a, Garuti & Friolo 1978/79) that characterize the protoliths adjacent to the mylonitic shear zones investigated here.

Rift-related structures in the Ivrea–Verbano Zone include the shear zones described below and have been mapped over an area of several hundred square kilometers (Brodie & Rutter 1987*a*; Handy 1987; Handy & Zingg 1991). Anastomozing, amphibolite to granulite facies, mylonitic shear zones accommodated extension parallel to the main foliation which follows the arc of the Ivrea–Verbano Zone. These shear zones are more common in the northeastern part of the Ivrea–Verbano Zone, where thermobarometric data indicate the greatest amount of crustal thinning (Handy *et al.* 1999). The most

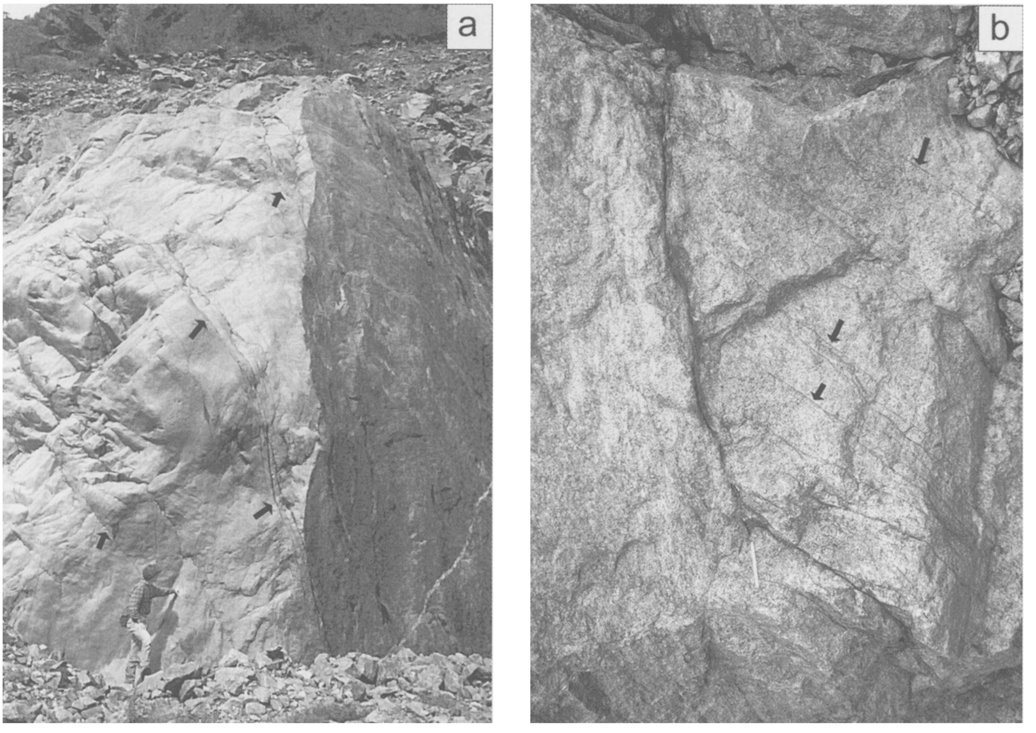

Fig. 3. Shear zones in lherzolite of the Balmuccia ultramafic body. (**a**) Type 2 shear zones appear as elongate cracks (arrows) and have conjugate orientations. The dark surface to the right is the serpentine-coated surface of such a shear zone. (**b**) Termination of a type 2 shear zone marked by discordant splays and late pseudotachylite (match tip). Type 1 shear zones (arrows) are truncated by the type 2 shear zone. Match for scale is 5 cm long.

prominent Early Mesozoic extensional structure is the Pogallo Shear Zone (PSZ in Fig. 1a), a 1–3 km wide mylonitic belt which accommodated sinistral, noncoaxial shear under retrograde amphibolite to greenschist facies conditions within quartz-rich metasediments. We shall discuss the significance of these structures in the final section, but first analyse their temporal equivalents in the ultramafic bodies.

Structural geology of the shear zones

Shear zones in the Balmuccia peridotite are strikingly narrow (Fig. 3). They comprise intricate strands of planar and arcuate, crack-like shear zones ranging in width from less than a mm to a few cm at most. Most of our observations were made in a quarry just above the road between the towns of Balmuccia and Bottorno, flanked by the northern bank of the Sesia river (locations indicated by stars in Fig. 2). It is unfortunate that the quarry has been active intermittently over the years, so that some of the outcrops reported in this paper no longer exist.

Two types of shear zone can be discerned (Figs. 3a, b). (1) Black shear zones form individually or as conjugate pairs which are truncated by later shear zones (Fig. 3b) and oriented at 45° to 60° to the pre-existing compositional banding (Fig. 4a). These shear zones contain microstructural evidence for viscous creep of olivine and pyroxenes, as described below. (2) Dark green to white, serpentine- and chlorite-bearing shear zones form long (one to several meters, Fig. 3a), generally planar strands that strike approximately N–S and dip subvertically (Fig. 2). These type 2 shear zones contain a very fine grained mylonitic foliation that is defined by aligned serpentine and chlorite grains. At their ends, these shear zones arc at high angles to the pre-existing foliation (Figs 2, 3b), often terminating as horsetail splays several cm to dm from the host strand.

Type 2 shear zones truncate and overprint type 1 (Fig. 3b), and are therefore clearly younger than the latter. Indeed, the high grade assemblages in the type 1 shear zones are rarely well

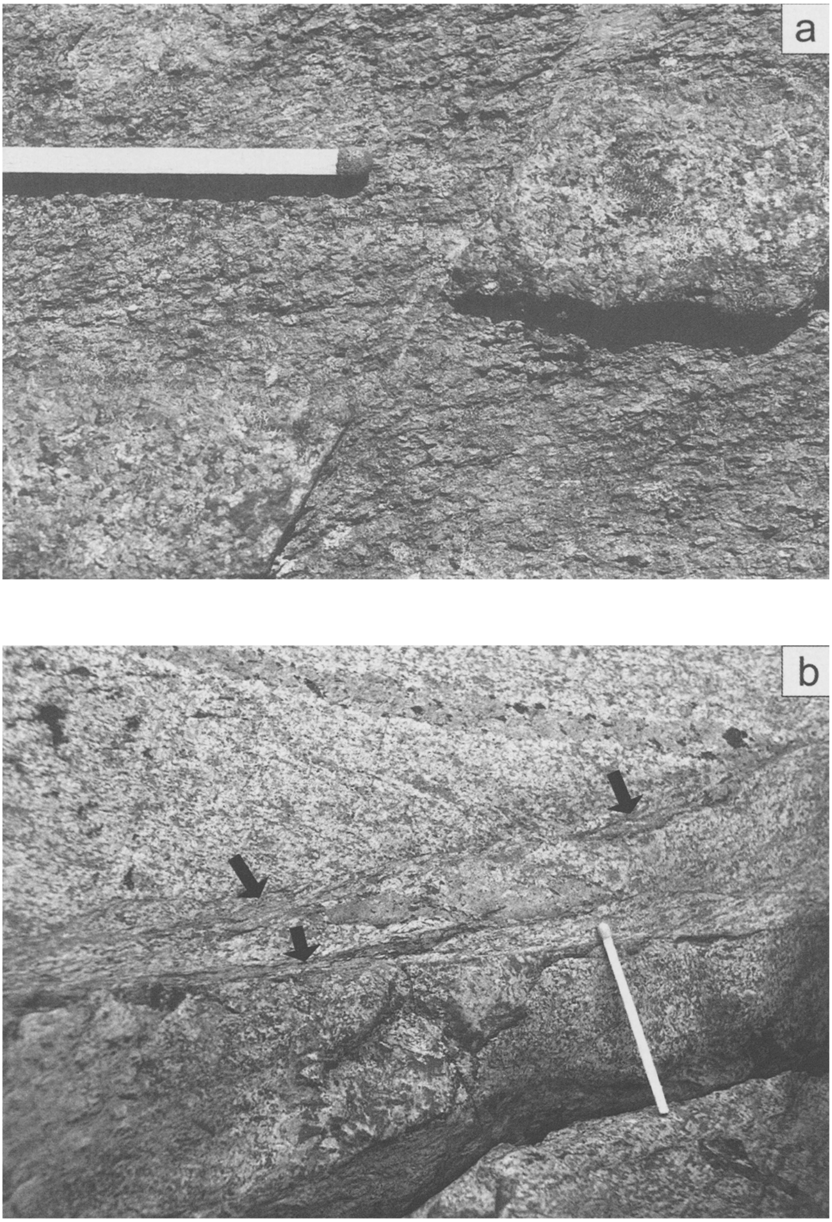

Fig. 4. Type 1 shear zones. (**a**) Shear zone offsets cumulate pyroxenite layer. Match for scale is 5 cm long. (**b**) Shear zones defined by closely spaced mylonitic foliation (arrows) truncates granulite facies schistosity and is related to vein-type pseudotachylite (above match tip).

preserved, as they usually show various degrees of brittle overprinting. This overprint takes the form of tectonic breccia or locally even pseudotachylite and ultracataclasite.

The displacement along both types of shear zone rarely exceeds a few centimeters (Fig. 4a), although the cumulative displacement along several strands making up type 2 shear zones is often a meter or more. The shear zones are spatially associated with vein-type pseudotachylites (Fig. 4b), some of which contain mineralogical evidence for formation under granulite facies conditions (Obata & Karato 1995). Most pseudotachylites, however, cut both types of shear zones and are clearly related to late, discordant cracks.

The type 1 shear zones and associated pseudotachylites have received considerable attention over the past twenty-five years (Garuti & Friolo 1978/79; Skrotzki *et al.* 1990; Obata & Karato 1995; Jin *et al.* 1998), and similar occurrences have been described from other ultramafic bodies further to the northeast in the Ivrea–Verbano Zone, especially in the Finero body (Kruhl & Voll 1978/79; Brodie 1980; Handy 1989) and the Premosello body (Rutter & Brodie 1988). Debate has centered on both the age of the shear zones (Variscan, Early Permian or Jurassic?) and on the mechanisms of strain localization leading to their growth: reaction-enhanced weakening (Brodie 1980); geometric softening of olivine (Obata & Karato 1995); dynamic recrystallization coupled with a transition to diffusion-accommodated grain-boundary sliding in olivine (Rutter & Brodie 1988; Jin *et al.* 1998); or a combination of these mechanisms (Handy 1989) have been proposed as possibilities. We first address the issue of localization before turning to the age of mylonitic shearing and the implications thereof for lithospheric extensional faults.

Microstructures and mineral assemblages

High temperature

To help resolve the debate on the mechanisms of strain localization in the upper mantle, we examined a remarkably well-preserved example of a type 1 shear zone in a spinel lherzolite (Fig. 4a). This shear zone is only 0.5 mm wide and offsets a magmatic pyroxenite band by 3.8 cm. As this magmatic band is oriented at 60° to the shear zone, the finite strain determined from the width and displacement is $\gamma = (380\,\mathrm{mm}/0.5\,\mathrm{mm})\cot 60° = 75$. Despite the minor displacement, this shear strain is almost an order of magnitude greater than the shear strains determined across larger natural shear zones (e.g. Grocott & Watterson 1980) or experimental shear zones in high pressure experiments (e.g. Schmid *et al.* 1987; Paterson & Olgaard 2000). Our sample is therefore a good natural laboratory for studying high-strain microstructures in upper mantle rock.

Regarded in thin section, the type 1 shear zone cuts both the foliation and individual grains in the spinel lherzolite protolith along sharp, uneven boundaries (Fig. 5b). The shear zone contains a very fine grained matrix that envelops rounded clasts of olivine (ol), clinopyroxene (cpx), orthopyroxene (opx) and spinel (sp) (Fig. 5b). The clasts are obviously derived from the lherzolitic and pyroxenitic protoliths.

The matrix has a weak foliation defined by microscopic laminae that are oriented parallel to subparallel to the shear zone boundaries. Locally, these laminae are buckled and form intrafoliational folds. The laminae have contrasting grain sizes and, as observed in backscattered electron (BSE) images (Fig. 6), also have different compositions. Fine-grained (10–30 μm) laminae of pure olivine (ol) and of pure clinopyroxene (cpx) alternate with even finer grained (0.5–6 μm) layers of a mixture of plagioclase (plag), hornblende (hbl), olivine (ol), clinopyroxene (cpx), and orthopyroxene (opx; Fig. 6a–d). The mixed layers extend from, or envelop, spinel and cpx porphyroclasts (Fig. 6b, c). In the transmission electron microscope (TEM), the phases in the mixed layers have a grain size as small as 0.2 μm. The small grains are usually dislocation free (Fig. 7a). The shapes of the individual phases do not vary systematically from grain to grain. This invariance of grain shape, the lack of dislocations, the very small grain size, and the dispersed distribution of these phases within the aggregate are all attributes which suggest that deformation involved viscous grain boundary sliding, probably accommodated by diffusional mass transfer along grain boundaries.

The laminae of pure ol and, more rarely, of pure cpx grains in the mylonitic matrix of type 1 shear zones occur in the vicinity of ol and cpx porphyroclasts. The matrix grains range in diameter from 10 to 30 μm and have formed by progressive dynamic recrystallization of these porphyroclasts. Olivine grains in these matrix laminae have moderate dislocation densities ($\sim 10^{14}\,\mathrm{m}^{-2}$) and show well-organized subgrain boundaries (Fig. 7b). This TEM observation, together with core mantle structures observed in the optical microscope, are diagnostic of subgrain rotation recrystallization (Poirier & Nicolas 1975). The matrix grains with high angle boundaries are generally subequant but locally have lobate grain boundaries, indicating that some grain boundary migration recrystallization also occurred.

The ultrafine-grained plag–hbl–cpx–opx–ol layers display a weak shape preferred orientation subparallel to the shear zone boundary defined by the margins of the large cpx and spinel grains (Fig. 6c). In most bands, however, the grains are equant and have rather straight boundaries. Some hbl/cpx phase boundaries are coherent, stepped boundaries along the *b*- and *a*-axes of both minerals (Fig. 7c). The heterogeneous distribution of grains and presence of

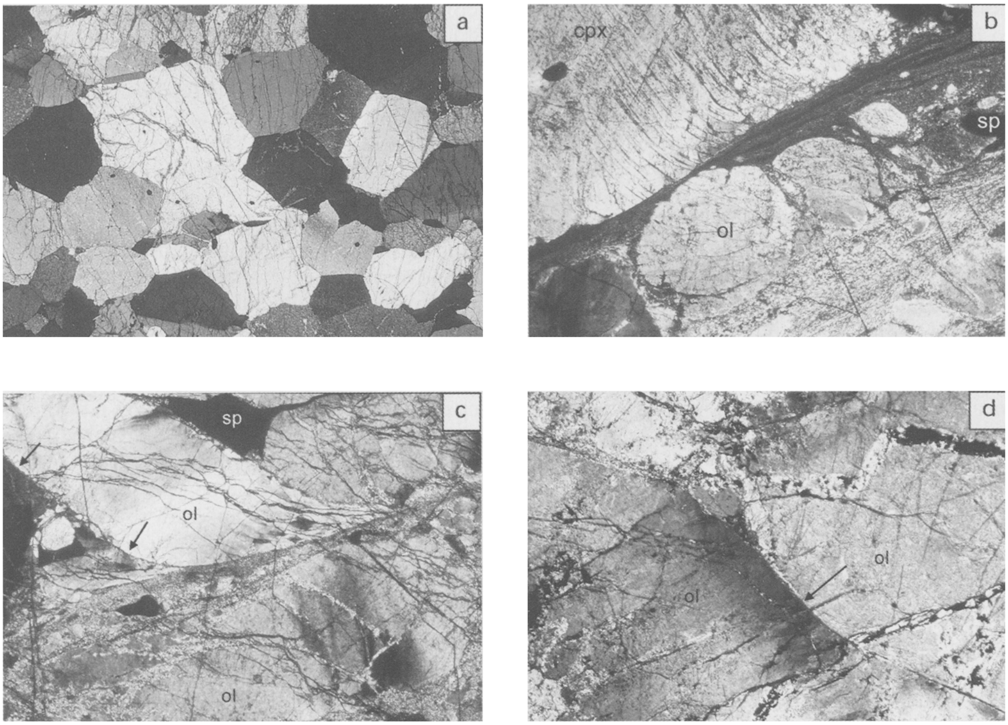

Fig. 5. Microstructures of a type 1 shear zone and its host rock, as observed in a polarizing light microscope with crossed nichols in the XZ fabric plane. (**a**) Protogranular microstructure of the host spinel lherzolite (frame length = 11.5 mm). (**b**) Thin mylonitic band at edge of shear zone in Fig. 4a. Note truncated twins in clinopyroxene (cpx), rounded clasts of olivine (ol), and spinel (sp) in ultrafine grained matrix of olivine, plagioclase, and hornblende (frame length = 1.35 mm). (**c**) Mylonitic microstructure in shear zone depicted in Fig. 4a. Arrows point to one of several arcuate cracks emanating from the side of the shear zone (frame length = 3.4 mm). (**d**) Close up of tip of crack in olivine grain indicated by arrows in (**c**), (frame length = 1.35 mm). Note undulose extinction adjacent to the crack.

coherent boundaries indicate that clinopyroxene and pargasitic hornblende coexisted stably in these layers.

Thus, the ol and cpx within the microscopic laminae of the mylonitic matrix are interpreted to have formed by different mechanisms. Pure ol and cpx layers (10–30 μm) derived from the dynamic recrystallization of ol and cpx porphyroclasts, whereas very small ol and cpx grains (0.5–6 μm) in plag–hbl–cpx–opx–ol layers were engendered by synkinematic mineral reactions.

The size and shape of the clasts within the matrix vary with their mineralogy. Spinel porphyroclasts are rounded and/or elongate and boudinaged, and are replaced by phase mixtures at their boundaries (Figs. 6b, c). Cpx and opx clasts are generally angular at the edges of the shear zone, rounded within the shear zone and have tails of dynamically recrystallized grains extending from their ends (Fig. 5b). Their internal microstructures are therefore interpreted to reflect the initial stages of deformation and localization, as discussed below.

Arcuate cracks emanate from the margins of the mylonitic matrix and terminate as inter- and transgranular fractures in the host rock (Figs. 5c, d). These cracks are unrelated to the late cracks mentioned above, as they are truncated by the latter and contain olivine and brown, pargasitic hornblende (Figs 6, 7). They therefore formed under the same high-grade conditions as the mylonitic matrix. The terminations of the cracks are oriented synthetically with respect to the bulk sinistral displacement along the shear zone boundaries. Displacement parallel to the crack boundaries increases from the crack tips (Fig. 5d) to their confluence with the mylonitic shear zone (Fig. 5c). Taken together, these observations indicate that the fractures opened as extensional shear fractures prior to and/or during viscous creep in the mylonitic matrix.

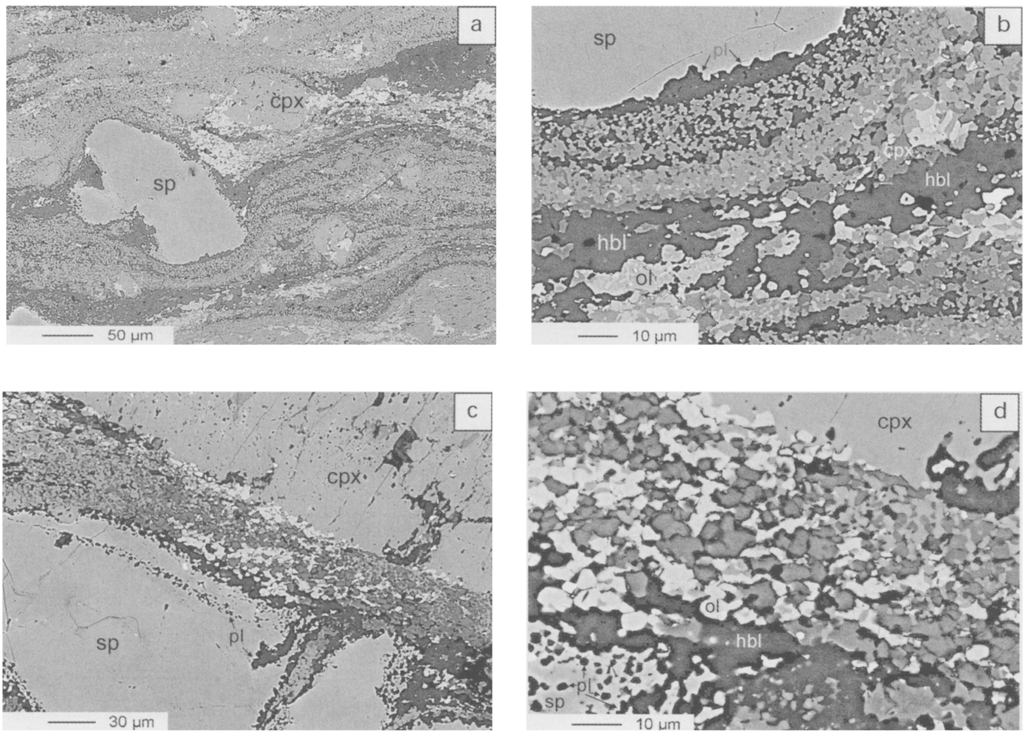

Fig. 6. Backscatter electron (BSE) images of mylonite in a type 1 shear zone. (**a**) Porphyroclasts of spinel (sp) and clinopyroxene (cpx) embedded in thin laminae of mixed phase layers consisting of olivine, plagioclase, orthopyroxene, clinopyroxene, and hornblende. (**b**) Detail of (**a**): boundary of a spinel grain (sp), where plagioclase (dark, pl), clinopyroxene (medium grey, cpx), and hornblende (slightly darker grey, hbl) form. The three new phases are well mixed. (**c**) A spinel grain (lower left, sp) and a clinopyroxene grain (upper right, cpx). Between these two grains is a thin mixed phase layer of plagioclase (pl), hornblende (hbl), olivine (ol), and clinopyroxene (cpx). (**d**) Detail of (**c**), showing the distribution of phases. plagioclase (dark, pl), olivine (lightest grey, ol), hornblende (darker grey, hbl), and clinopyroxene (lighter grey, cpx).

They appear to have propagated critically as inferred from their inter- and transgranular geometry, which is diagnostic of brittle intergranular and transgranular creep fracture (Gandhi & Ashby 1979).

Some fractures in the type 1 shear zones are kinematically related to small pull-apart structures that contain a glassy, former melt phase (Fig. 4b, see also Obata & Karato 1995). However, we do not think that deformation in the fine-grained mylonitic matrix described above involved melting because the thin layers of very fine-grained reaction products (plag, ol, hbl, cpx) alternate with monomineralic layers of dynamically recrystallized olivine. Dynamic recrystallization of olivine is indicative of lower strain rates than the seismic rates required to form pseudotachylite (e.g. Obata & Karato 1995), especially at the high temperatures of the deformation. The mylonitization in the matrix may have occurred during post-seismic creep, as described below.

Low temperature

The microstructure of type 2 shear zones is typically cataclastic, with fragments of altered, high-grade minerals floating in a ultrafine-grained, locally foliated matrix of serpentine and chlorite (Fig. 8). Evidence of this hydrous, greenschist facies overprint is also evident in type 1 shear zones, with transgranular serpentine-filled cracks cutting across the high grade matrix and porphyroclasts (Fig. 5c). Even in the mylonitic matrix of the type 1 shear zones, a fine-grained mixture of chlorite + magnetite ± serpentine forms pseudomorphs of former small spinel grains (Fig. 7d). These pseudomorphs indicate that the retrograde phase

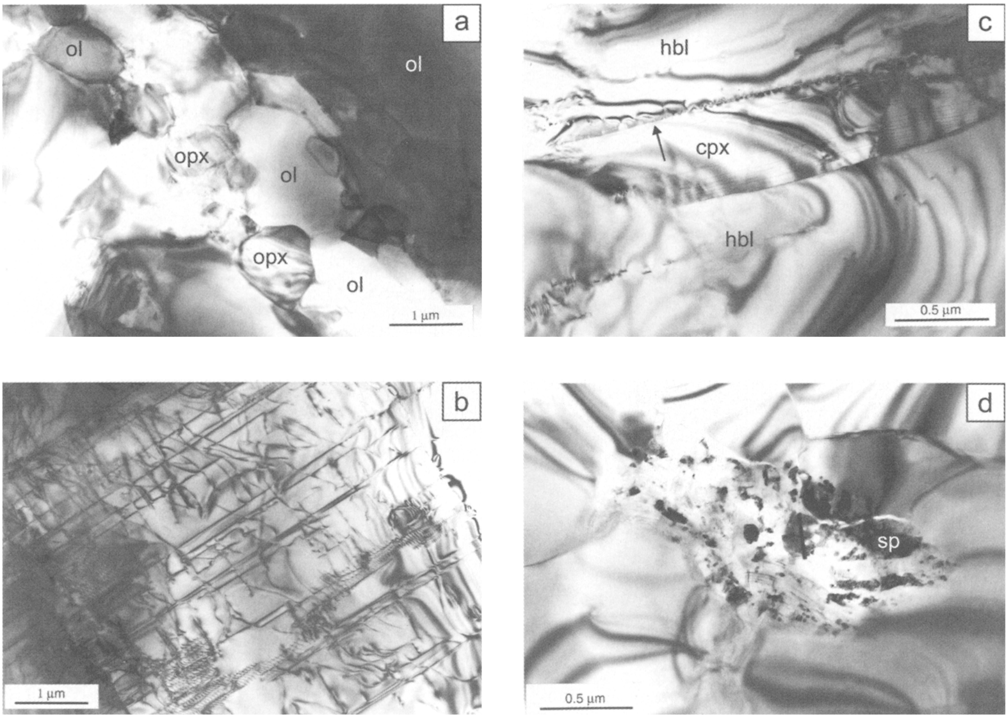

Fig. 7. Transmission electron microscope (TEM) images of mylonite in type 1 shear zone. (**a**) Olivine and opx grains in mixed phase laminae derived from spinel and cpx porphyroclasts. The very fine grains are dislocation-free and have equant shapes. (**b**) Dislocations within an olivine grain from a dynamically recrystallized monophase olivine layer (average diameter 20–50 µm) in the tail of an olivine porphyroclast. Note the well-organized subgrain walls. (**c**) View parallel to the *c*-axis of a clinopyroxene grain (oriented east-west in center) between two pargasitic hornblende grains. The upper boundary of the cpx grain (arrow) is coherent along the shared *a* and *b* crystallographic directions of cpx and hornblende. Mottled contrast along this boundary reflects steps in the coherent boundary. (**d**) Pseudomorphous replacement of spinel (sp) by an aggregate of serpentine, chlorite and magnetite. Small spinel aggregates are found in some of the pseudomorphous aggregates.

mixture grew after the high temperature deformation in type 1 shear zones.

Pressure–temperature conditions of type 1 shear zones

The BSE images of the very fine plag–hbl–cpx–ol layers in Figure 6 indicate that these phases all formed from the breakdown of spinel according to the discontinuous reaction:

$$sp + cpx + opx + H_2O = an + hbl + ol.$$

This syntectonic reaction and phase assemblage provides good constraints on the P–T conditions of deformation (Fig. 9). The spinel-lherzolite to plagioclase-lherzolite transition in the CFMASH ($CaO–FeO–MgO–Al_2O_3–SiO_2–H_2O$) system occurs at pressures between 400–750 MPa at temperatures of 700–1000 °C (Gasparik 1987; Bucher & Frey 1994; Furusho & Kanagawa 1999). This transition shifts to higher pressures at lower anorthite contents of the plagioclase, but there is almost no shift with pressure for anorthite contents between An_{80} to An_{100} (Gasparik 1987). EDS spectra of plagioclase grains in our samples taken with the SEM (the grains are too small to be analysed with the electron microprobe) indicate almost no Na and Si/Al ratios of approximately one, so that the anorthite content of the plagioclase is probably $\geq An_{90}$. Thus, pressures for the type 1 shear zones can be approximated with the CFMASH system, and the maximum pressure of the plagioclase lherzolite mylonite is about 600 MPa at 1000 °C (Fig. 9).

Chlorite was not stable during deformation, and therefore temperatures must have exceeded about 750 °C for the given low pressure range (chl-out curve, Fig. 9). The presence of pargasitic

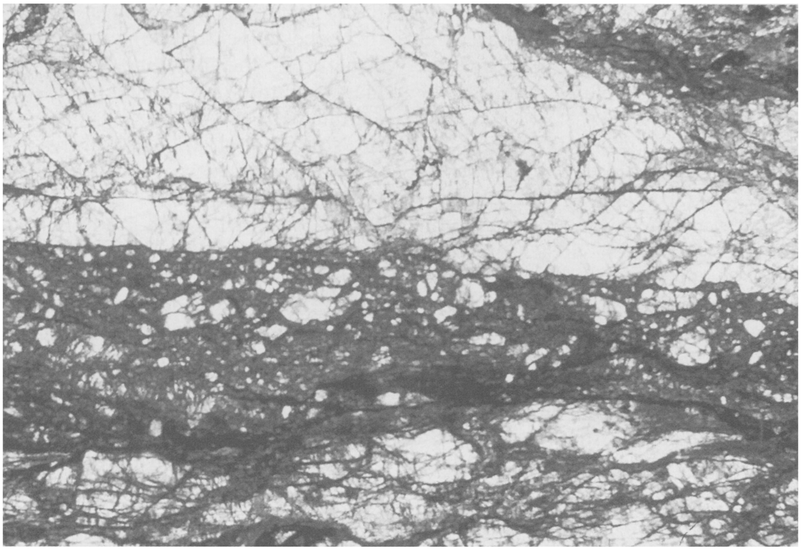

Fig. 8. Cataclastic microstructure of a type 2 shear zone. Note the angular, fractured clasts of partly serpentinized olivine (large clast at top, small clasts in matrix) and a nearly opaque matrix comprising mainly ultrafine grained serpentine and chlorite. View in the XZ fabric plane. Length of micrograph is 3.4 mm.

hornblende constrains the upper temperature limit of the stability field to an extent dependent on the bulk composition of the rock. The two experimental amphibole dehydration curves

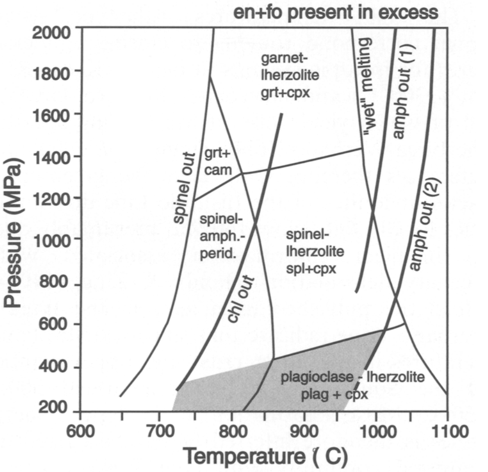

Fig. 9. P–T diagram for ultramafic rocks with the inferred pressure and temperature fields for the high-temperature shear deformation during Early Mesozoic rifting of the upper mantle. Stability fields and curves for stability of spinel and chlorite after Bucher & Frey (1994), experimentally determined hornblende stability curves from Wallace & Green (1991) (amph-out, 1) and Niida & Green (1999), (amph-out, 2). The probable maximum pressure and temperature range for the high temperature deformation of type 1 shear zones is indicated by grey shading.

correspond to MORB pyrolite compositions (Niida & Green 1999, amph-out (2) curve in Fig. 9) and to depleted mantle compositions (Wallace & Green 1991, amph-out (1) curve in Fig. 9). The Balmuccia composition lies between these two compositions (Sinigoi *et al.* 1994), so that the upper temperature limit of deformation was somewhere between 900 and 1000 °C. Deformation in type 1 shear zones therefore occurred within a maximum range of 750–1000 °C at pressures of 400–600 MPa (shaded area in Fig. 9). Similar pressures were inferred for shear zones in the Balmuccia peridotite by Obata (1976) and Walter & Presnall (1994).

The P–T conditions of strain localization within type 1 shear zones are consistent with conditions inferred for syntectonic microstructures in the pure olivine and clinopyroxene layers described above. Dynamic recrystallization of olivine in these layers constrains the temperature of deformation to have been at least 600–700 °C based on the extrapolation of laboratory flow laws for grain-size-insensitive power law creep of hydrous olivine to geological strain rates of 10^{-11}–$10^{-14}\,s^{-1}$ (Handy & Zingg 1991, references therein). The 10–30 μm diameter of dynamically recrystallized olivine grains from the coarser grained laminae of the mylonitic matrix is consistent with differential stresses ranging from 100–200 MPa according to the laboratory grain size piezometer of Van der Wal *et al.* (1993): $D = 0.015\Delta\sigma^{-1.33}$, where D and $\Delta\sigma$ are, respectively, the average grain diameter (in m) and differential stress (in MPa). These high differential stresses are only rough estimates but are consistent with the microstructural evidence that deformation in the sample occurred at the brittle-to-viscous transition.

The growth of pargasitic hornblende at the expense of clinopyroxene and in the presence of anhydrous reactants (sp, ol, cpx, opx) indicates that the reaction consumed water. The amount of water cannot have been great, however, given the small size and minor volume proportion of the hornblende grains.

The geodynamic significance of this syntectonic reaction is that strain localization in the type 1 shear zones was associated with a significant pressure drop. The spinel lherzolite that had equilibrated at a depth of about 34–44 km prior to localized shearing (Shervais 1979; Rivalenti *et al.* 1981, 1984; Sinigoi *et al.* 1994) was partly replaced by a plagioclase–hornblende lherzolite at shallower depths. Subsequently, the type 2 shear zones were active under hydrous greenschist facies conditions, probably at temperatures below 400 °C, in view of the stable mineral assemblage described in the previous section (Trommsdorff & Evans 1974; Trommsdorff 1983; Bucher & Frey 1994). Based on this information, a range of possible depths during deformation can be estimated from isotopic mineral cooling ages in the Ivrea–Verbano Zone and from a knowledge of geotherms in attenuating lithosphere. Accordingly, temperatures at the base of the attenuating Ivrea–Verbano Zone decreased from 800 °C to below 300 °C by Early to Middle Jurassic time (Handy & Zingg 1991 and references therein). At an assumed transient geothermal gradient of 30 °C/km during extensional shearing (e.g. Chapman 1986), these temperatures correspond to a depth range of 10–25 km for localized shearing in the Balmuccia peridotite.

Age of the shear zones

Neither the shear zones nor the pseudotachylites in the Balmuccia peridotite have been isotopically dated, partly because dating such small volumes of heterogeneous, fine grained aggregates with current techniques poses a formidable analytical challenge and is likely to generate ambiguous numbers. For now at least, the age of the type 1 and 2 shear zones can be constrained by considering the temperature estimates above in the context of published isotopic mineral cooling ages in the Ivrea–Verbano Zone.

The high temperature, type 1 shear zones are overprinted by, and therefore certainly older than the type 2 shear zones, but younger than the penetrative foliation and annealed microstructure in the spinel lherzolite host rocks. The main foliation and annealing in the host rocks are dated at 300–320 Ma by analogy with similar sub-solidus, high-grade structures in mafic rocks and metasediments in the Ivrea–Verbano Zone (Handy *et al.* 1999). Type 1 shear zones associated with high-grade pseudotachylites therefore post-date Variscan orogenesis. An Early Mesozoic (Late Triassic to Early Jurassic?) age for the type 1 shear zones and related pseudotachylites is likely in light of similar high-grade metamorphic conditions for mylonitic shear zones in the northeastern part of the Ivrea–Verbano Zone. There, the shear zones attenuate, and therefore post-date, isobars associated with 270–290 Ma magmatism and metamorphism (Handy *et al.* 1999). Furthermore, the petrological evidence in the type 1 shear zones for decompression and exhumation accords well with structural and petrological evidence in metabasic and pelitic rocks of the Ivrea–Verbano Zone for rapid cooling and E–W directed, extensional mylonitic shearing some 180–230 Ma (Handy & Zingg 1991). This extensional shearing is clearly related to the formation of Latest Triassic to Early to Middle Jurassic rift basins in the upper crust of the Southern Alps (Handy 1987).

The ≤400 °C temperatures for the type 2 shear zones correspond roughly to closing temperatures for isotopic systems in biotite (K-Ar, Rb-Sr, *c.* 300 °C) and muscovite (K-Ar, *c.* 350 °C), all of which yield 160–220 Ma cooling ages in the Ivrea–Verbano Zone (Zingg *et al.* 1990 and references therein). Only near the greenschist facies mylonites of the Insubric Line do biotite ages locally fall below 160 Ma, presumably due to incipient chloritization associated with Tertiary deformation (Handy & Zingg 1991). Thus, the published mica ages in the Ivrea–Verbano Zone indicate that since 160 Ma, temperatures in the lower crust and upper mantle of the Southern Alps never exceeded 300–350 °C. Most deformation in the type 2 shear zones is therefore inferred to have occurred in temporal continuity with type 1 shear zones during Early Mesozoic rifting. However, given the proximity of the Balmuccia ultramafic body to the Tertiary Insubric Line (Fig. 1a) and the brittle overprint of many type 1 and 2 shear zones, we cannot rule out that some type 2 shear zones were reactivated during Tertiary time. Indeed, with the exception of pseudotachylites related to type 1 shear zones, most pseudotachylites in the Ivrea–Verbano Zone are interpreted to have formed in response to

Oligo-Miocene, oblique backthrusting along the Insubric Line (Zingg *et al.* 1990; Techmer *et al.* 1993).

To summarize, both type 1 and type 2 shear zones are believed to have formed during a single deformational event related to rifting in Early Mesozoic time. However, Tertiary (Alpine) reactivation of some type 2 shear zones cannot be ruled out.

Discussion

Micromechanisms of strain localization

We interpret the type 1 and 2 shear zones in the Balmuccia ultramafic body to represent two successive stages of strain localization during rifting of the continental lithosphere of the Southern Alps in Early Mesozoic time. During stage 1, extensional shear fracturing under granulite facies conditions triggered the nucleation of ultrafine-grained mylonitic shear zones. This strain-dependent brittle-to-viscous transition is inferred to have occurred rapidly and in the presence of only minor amounts of fluid. The total amount of fluid introduced to the shear zones and contained in pargasite is estimated to be of the order of 0.1 wt% H_2O. The transition involved the spontaneous nucleation of lower pressure minerals (plag, hbl) along cracks and dilatant grain boundaries of the higher pressure phases (sp, cpx). Critical crack growth was therefore intimately related to the nucleation of minerals with larger molar volumes than the higher pressure phases which they replaced.

During stage 2, strain concentrated within very long, narrow shear zones at low angles to the pre-existing foliation and subparallel to the extensional shearing plane. As discussed in the next section, these presently subvertical shear zones were originally subhorizontal to moderately dipping during Early Mesozoic extension. Localization involved the breakdown of olivine, pyroxene and hornblende to form the hydrous phases serpentine and chlorite in the fine-grained mylonitic matrix as well as in parts of the undeformed rock adjacent to the mylonites. This testifies to a significant influx of fluids during the latter stages of extensional deformation. Like the type 1 shear zones before, strain localization in the type 2 shear zones was closely related to dilatancy and syntectonic phase transformations in the presence of a hydrous fluid phase.

Figure 10 shows a possible strength evolution for the two stages of strain localization outlined above. This evolution is speculative, based as it is on a correlation of microstructures in our samples with experimental microstructures and rheologies obtained at high temperatures and laboratory strain rates (Paterson 1987). Nevertheless, it serves as a qualitative guide to the strain-dependent behaviour of the upper mantle during rifting.

The stress–strain curve in this figure pertains to the entire volume of rock affected by deformation (i.e. the host lherzolite plus fractures and

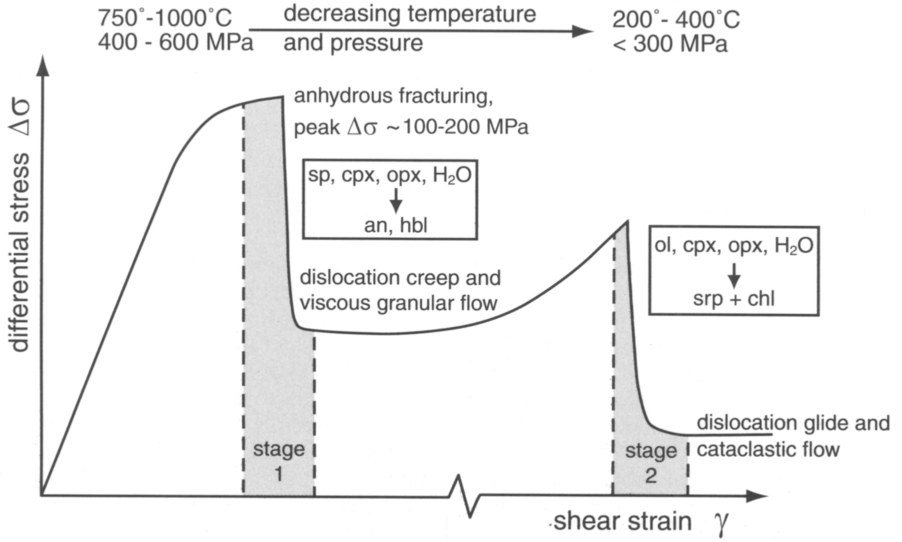

Fig. 10. Schematic strength versus strain evolution of lherzolite in the Balmuccia ultramafic body during Early Mesozoic rifting inferred from microstructures (see text).

shear zones). An initial increase in stress just prior to fracturing is inferred from traces of low strain intracrystalline plasticity adjacent to fractures in the olivine grains of the wall rock (Fig. 5d). Peak strength then coincided approximately with fracturing during the formation of the type 1 shear zones (Fig. 10). Fracturing marked the onset of the spinel- to plagioclase-lherzolite transition, which is limited to the immediate vicinity of the fractures. The fracturing increased permeability which in turn enhanced fluid infiltration. The interconnection of these fractures lined with very small strain-free grains drastically weakened the deforming rock, indicated in Figure 10 by a marked strength drop. This strength drop is inferred from numerous experimental and theoretical studies showing that significant weakening is induced by dynamic recrystallization (Zeuch 1982, 1983; Tullis & Yund 1985; see de Bresser *et al.* 2001 for a recent discussion) and, more importantly, by a transition to diffusion or reaction-accommodated viscous granular flow (e.g. White & Knipe 1978; Stünitz & Tullis 2001). These mechanisms were detected in the mylonitic laminae of the type 1 shear zones, and have been recognized in gabbroic mylonites (Brodie & Rutter 1985; Stünitz 1993; Kruse & Stünitz 1999) as well as in peridotitic mylonites (Boullier & Guegen 1975; Newman *et al.* 1999; Furusho & Kanagawa 1999). The high differential stress range (100–200 MPa) estimated from the small sizes of dynamically recrystallized olivine grains was probably transient, and marked a short period of rapid slip parallel to the shear zone boundaries during and/or immediately after macroscopic failure at peak strength. The growth of the mylonitic matrix may have stabilized the deformation at a stress significantly lower than the peak strength recorded by the observed grain size of dynamically recrystallized olivine (Fig. 10).

It is interesting to note that strain partitioning within very fine-grained mylonitic microstructures like those observed in our samples has been produced in the laboratory at similarly high temperatures (900 °C) and high strain rates ($\gamma = 5 \times 10^{-5}\,s^{-1}$: Stünitz *et al.* 1999) in similar lithologies. This lends credence to the idea that the mylonitic matrix deformed at very high strain rates and is related to the formation of pseudotachylite in nearby pull-apart structures (Fig. 4b).

Continued shearing at decreasing temperature and lithostatic pressure may have induced non-linear work-hardening (Fig. 10) due to the exponential (Arrhenius) dependence of viscous creep strength on temperature (Weertman 1970). However, the rock is inferred to have weakened again when serpentine and chlorite nucleated and grew at the expense of the high-grade minerals (Fig. 10). Laboratory experiments indicate that serpentinite (Raleigh & Paterson 1965) has a laboratory strength several orders of magnitude less than the strengths of olivine and pyroxenes at comparable homologous temperatures and strain rates (Fig. 1 in Brodie & Rutter 1987*b*). Below about 500–600 °C, olivine aggregates undergo cataclasis, even at low strain rates and very fine grain sizes (Handy 1989; Handy & Zingg 1991), whereas sheet silicates deform by dislocation glide and/or creep parallel to their 001 surfaces (e.g. biotite: Wilson & Bell 1979; Kronenberg *et al.* 1990) at natural strain rates and temperatures down to 150–250 °C (Lin 1997). On the crustal scale, the prime agent of weakening is inferred to have been the interconnection of the type 2 shear zones to form an anastomozing network subparallel to the extensional shearing plane. This is consistent with the observation above that most displacement was accommodated by type 2 shear zones.

The scenario above for the shear zones of the Balmuccia ultramafic body obviously does not preclude other strain localization mechanisms previously proposed for ultramafic rocks in the Ivrea–Verbano Zone. Indeed, a localization mechanism proposed for all occurrences so far is a strain-induced switch in deformation mechanisms for olivine from dislocation creep to viscous granular flow accommodated by grain boundary diffusion (Premosello body, Rutter & Brodie 1988; Balmuccia body, Jin *et al.* 1998) or syntectonic reaction (Finero body, Handy 1989). Yet, in all these studies pre- to syn-mylonitic fracturing and cataclasis have been either overlooked or attributed solely to late-mylonitic or post-mylonitic deformation under hydrous, sub-greenschist facies conditions.

Our study underscores the importance of combined fracturing and syntectonic metamorphism as a most effective agent of strain localization in the upper mantle (Vissers *et al.* 1997). Moreover, it confirms the predictions of Drury *et al.* (1991) that hydrous brittle deformation in the upper mantle localizes at temperatures less than 900 °C. We note that the weakening associated with coeval fracturing and heterogeneous nucleation of transiently fine-grained reaction products is stress- and strain-induced and occurs within an initially very strong lithology. Induced weakening therefore differs fundamentally from weakening which results from the localization of mylonitic deformation within pre-existing weak lithologies (Ranalli & Murphy 1987) or inherited structures, as proposed for natural mylonites (granitic mylonites: Segall & Pollard 1983, Segall & Simpson 1986; gabbro: Stünitz 1993; abyssal peridotite: Jaroslow *et al.* 1996) and as demonstrated in experiments (Tullis *et al.* 1990).

Despite their importance for localizing deformation in the upper mantle, type 1 shear zones are rarely preserved in naturally deformed peridotites. Due to overprinting during retrograde stage 2 deformation, the initial high temperature assemblages and microstructures of the type 1 shear zones are only preserved in narrow, 'arrested' zones of minor displacement at the margins and near the ends of the type 2 shear zones (Fig. 3b).

Implications for lithospheric extensional faulting and weakening

Induced weakening of the upper mantle potentially determines the large-scale structure and rheology of continental margins. The most striking consequence of the two-stage strength evolution outlined above is that the lithosphere may have weakened most where extrapolated experimental flow laws (e.g. as employed by Ranalli & Murphy 1987) indicate that it was initially strongest, *viz.*, at the top of the lithospheric mantle. Fault rocks formed there evidently have microstructures and rheologies which changed with strain during exhumation. To assess these effects on the lithospheric scale, we briefly review Early Mesozoic extensional structures in the Ivrea–Verbano crustal section, as shown in map view in Figure 1a and in the restored section in Figure 11.

Previous studies in the Ivrea–Verbano Zone have shown that rift-related attenuation of the lithosphere was accommodated primarily in quartz-rich granitoid and pelitic rocks within the Pogallo Shear Zone (Handy 1987; Handy & Zingg 1991), at the base of the intermediate crust (Fig. 11). The PSZ comprises retrograde amphibolite to greenschist facies mylonites, with cataclasites at its upper limit marking the Early Mesozoic, viscous-to-brittle transition in the crust (Handy 1987). Related mylonitic shearing also overprinted granulite facies metabasites and metasediments within the former lower crust in the Ivrea–Verbano Zone (Brodie & Rutter 1987*a*; Zingg *et al.* 1990). Comparison of pre- and post-rift crustal thicknesses from thermobarometric data at the northeastern end of the Ivrea–Verbano Zone indicate that the PSZ and lower crustal shear zones together

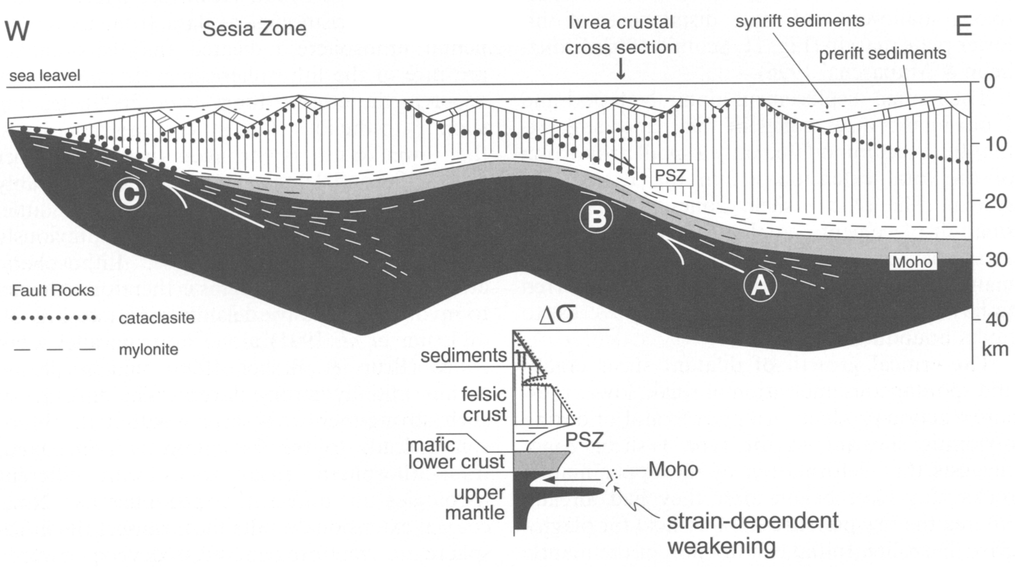

Fig. 11. Schematic cross section through the Apulian margin of Tethys at the end of Early Mesozoic rifting (after Handy & Zingg 1991; Schmid 1993). A, location for nucleation of type 1 shear zones; B, location for activity of type 2 shear zones; C, trans-lithospheric shear zone exhuming subcontinental mantle to the ocean floor. Approximate location of present Sesia Zone is labelled. Geometry of rift basins adopted from the references above. PSZ, Pogallo Shear Zone, as in Fig. 1a. Strength versus depth diagram below shows relative strength of lithospheric layers beneath the downward arrow, corresponding to the Ivrea crustal section. Note the horizontal, leftward arrow just below the Moho, indicating strain weakening described in the text.

excised a total of 20–25 km of crust in Early Mesozoic time (Handy *et al.* 1999).

Regarded on the lithospheric scale, these extensional structures are interpreted by some authors to be part of an asymmetrical rift system, with the lower crust and upper mantle of the Apulian margin, represented here by the Ivrea–Verbano Zone exposed in the lower plate of a uniform-sense master fault dipping to the west beneath the opposite European margin (Lemoine *et al.* 1987; Stampfli & Marthaler 1990; Vissers *et al.* 1991; Favre & Stampfli 1992; Froitzheim & Manatschal 1996). Unfortunately, this purported master fault is not exposed, either because it never existed or because Alpine overprinting of rift-related structures in the deep parts of the opposite European margin (all of which are located north and west of the Insubric Line in Fig. 1) was so complete. However, field studies clearly show that currently exposed Early Mesozoic shear zones were originally E-dipping (i.e. toward the rifted Apulian margin), both in the Ivrea–Verbano Zone and in the lower Austro-Alpine Margna-Sella units (Müntener & Hermann 2001). Together, these shear zones are inferred to have exhumed lower crustal and subcontinental, upper mantle rocks, as depicted in Figure 11 (Handy 1987; Handy & Zingg 1991). The Strona-Ceneri and Sesia Zones adjacent to the Ivrea–Verbano Zone (Fig. 1) formed, respectively, shallower and more distal parts of this lower plate margin (Fig. 11, Schmid 1993; Froitzheim & Manaschal 1996).

The limited displacement along the type 1 and 2 ultramafic shear zones in this paper suggests that they accommodated only a small proportion of the total extension within this extensional system. The type 1 shear zones are therefore small-displacement analogues for incipient extensional detachment faults in the uppermost mantle (A in Fig. 11), some of which are inferred to have connected upwards through the crust to faults bounding rift basins.

The critical growth of dilatant shear cracks and spontaneous nucleation of weak, lower pressure reaction products just prior to and/or during mylonitic shearing in the type 1 shear zones suggests that deformation of the upper mantle rocks may have begun after they had already entered the low pressure stability field for plagioclase lherzolite. Initial exhumation of the mantle must therefore have occurred within the overlying crust, along the Pogallo Shear Zone. The juxtaposition of hot mantle rock with cooler crustal rocks is reflected in the contrasting P–T paths for the mantle and crustal rocks in the Ivrea–Verbano Zone. While the exhuming mantle rocks underwent pronounced cooling (Fig. 9), the overlying crustal rocks were initially heated by these relatively hot mantle rocks in the footwall (Fig. 3c in Handy *et al.* 1999).

During this initial stage of exhumation, the upper mantle was stronger than the overlying crust (initial strength profile for the upper mantle in Fig. 11) and is inferred to have acted as a stress guide. Differential stress within this layer increased until it attained the fracture strength of upper mantle rock. Fracturing allowed the ingress of fluids and facilitated the phase changes which led to pronounced weakening in the type 1 shear zones. With continued stretching, a massive influx of fluids and the coalescence of serpentinitic, type 2 shear zones (B in Fig. 11) effected further weakening of the upper mantle. At this stage, the strength of the upper mantle is inferred to have dropped below that of the lower crust, as indicated by the arrow just below the Moho on the strength versus depth diagram in Figure 11.

The scenario above has several implications for the evolution of rifted continental margins. First, the lower crust is ultimately the strongest rather than the weakest layer and exceeds the strength of the upper mantle just beneath the Moho (Handy 1989). This is at odds with many models that incorporate a weak lower crust and strong upper mantle (e.g. Chen & Molnar 1983; McKenzie *et al.* 2000). However, a recent reassessment of seismological data from the continental lithosphere indicated that earthquakes are rare in the lithospheric mantle and usually occur in the crust (Maggi *et al.* 2000), lending support to the idea that, at least in some places, the lower crust is stronger than the upper mantle. Second, large extensional faults probably root within the top of the lithospheric mantle, rather than within the lower crust as previously proposed (e.g. Reston 1990). Lithospheric attenuation in rifted margins is therefore inferred to involve progressive delamination (see Fig. 3b of Lister *et al.* 1991) along layer-parallel weak zones (Brun & Beslier 1996) that nucleated within initially strong layers. The linkage of such strong-then-weak layers within the lithosphere leads to the formation of noncoaxial, trans-lithospheric shear zones with different rheologies in different depth-intervals. Noncoaxial extensional faults that transect the lithosphere are therefore believed to develop towards the end of rifting, rather than at the beginning as proposed by Wernicke (1985). Third, the formation of trans-lithospheric shear zones with very weak fault rocks in the distal parts of rifted margins (C in Fig. 11) is predicted to reduce the overall strength of the attenuating crust and therefore to accelerate rifting. Indeed, Vissers *et al.* (1995) have pointed out that the development of one or more through-going extensional shear zones may be responsible for increased spreading velocity in the Liguro-Piemontese domain from pre-middle Jurassic values of 0.5 cm/a to 2 cm/a from the middle Jurassic breakup onwards (Savostin *et al.* 1986). Finally, trans-lithospheric shear zones comprising weak, serpentinic mylonites and cataclasites in their shallowest segments (C in Fig. 11) may be responsible for the exhumation of subcontinental lithospheric mantle in continent–ocean transitional domains as observed, for example, in submarine surveys of the non-volcanic Galicia margin off the coast of Spain (Boillot *et al.* 1995).

Inclined extensional shear zones like those depicted in Figure 11 are not necessarily diagnostic of uniform sense simple shear (Wernicke 1985), but can be interpreted as localized noncoaxial shear of distal parts of the rifted continental margin within an overall regime of lithospheric scale pure shear (Brun & Beslier 1996). This scenario was first proposed for the latter stages of rifting of the lower plate Apulian margin by Handy (1987) and contrasts with other reconstructions of the Apulian margin in which lithospheric attenuation was accommodated solely by simple shear along uniform-sense master faults dipping either to the east (Trommsdorff *et al.* 1993) or west (e.g. Froitzheim & Manatschal 1996). In scaled analogue models of rheologically stratified, continental lithosphere subjected to vertical shortening and lateral, pure shear extension, Brun & Beslier (1996) showed that rheological instabilities within an initially stiff upper mantle layer induced asymmetrical rift geometries, such that a conjugate set of non-coaxial, extensional shear zones developed at the base of the lithosphere. Inserting weaker material at the top of the lithospheric mantle accentuated this asymmetry, favouring the further growth of one of these non-coaxial shear zones to accommodate rapid extensional exhumation of subcontinental mantle rock in its footwall, as modelled by Callot *et al.* (2001). The strikingly similar geometries of the rifted margins in the scaled models with the reconstructed Tethyan passive margins suggests that strain-dependent weakening at the top of the lithospheric mantle may well have facilitated extensional exhumation of the subcontinental mantle.

Conclusions

The ultramafic shear zones within what was originally the deepest part of the Ivrea–Verbano Zone (northern Italy) formed at or near the Moho during Early Mesozoic rifting of the non-volcanic, Apulian continental margin. They accommodated only small displacements and are therefore regarded as examples of incipient extensional detachment in the subcontinental mantle.

Two types of shear zones with different mineral parageneses and deformational microstructures formed during successive stages of extensional exhumation of the subcontinental mantle. (1) Shear zones at moderate to high angles to the pre-existing foliation in the host spinel lherzolite involved strain localization by initial fracturing transitional to viscous granular flow under retrograde, high temperature conditions. (2) Very long, narrow cataclastic shear zones coated with serpentine and chlorite accommodated most of the extensional strain under hydrous, low temperature (greenschist facies) conditions. These shear zones are oriented at low angles to the pre-existing foliation.

In type 1 shear zones, brittle–viscous shearing coincided with pronounced decompression, as inferred from the syntectonic replacement of a high-pressure assemblage (ol–cpx–opx–sp) by an hydrous lower pressure (ol–plag–hbl) assemblage. Phase equilibria constrain this reaction to have occurred at 750–1000 °C at pressures of 400–600 MPa. Syntectonic decompression is consistent with widespread evidence in the Ivrea–Verbano Zone for marked cooling and exhumation of the Apulian continental margin in Early Mesozoic time. The dominant deformation mechanism in the ultrafine-grained reaction products is inferred to have been viscous grain boundary sliding, probably accommodated by diffusional mass transfer along the grain boundaries.

The strain-dependent changes in mineralogy and deformation mechanisms above are believed to have decreased ultramafic rock strength by at least an order of magnitude from its peak value of about 100–200 MPa just after the onset of fracturing. These rocks weakened even further once type 2 shear zones containing serpentine and chlorite coalesced subparallel to the bulk extensional shearing plane.

Our findings suggest that extensional detachments nucleate as cracks at or near the top of the, initially hard, upper mantle. There, ultramafic rocks weaken with strain as grain size is reduced by cataclasis and heterogeneous nucleation of very fine-grained reaction products. The upper mantle therefore evolves into a low viscosity detachment layer sandwiched between stronger mafic lower crust above and mantle below. In the case of the Apulian continental margin, the interconnection of several such detachment layers to form large, non-coaxial extensional fault zones may have caused the observed Mid-Jurassic increase in rifting rate between Europe and Apulia. Such weak faults zones may also have accommodated extensional exhumation of subcontinental Apulian mantle within the continent-ocean transition zone.

The very constructive reviews of F. Gueydan and K. Kanagawa as well as editorial comments by H. de Bresser significantly improved the manuscript. Thanks also go to J. Babist for field assistance, and to B. Ernst and M. Grundmann for helping to prepare the figures. We acknowledge the support of the German Science Foundation (grant Ha 2403/5-1 to MH) and the Swiss National Science Foundation (grants 2000-055420.98/1 and 2100-057092.99/1 to HS).

References

BOILLOT, G., AGRINIER, P. *ET AL.* 1995. A lithospheric syn-rift shear zone at the ocean-continent transition: preliminary results of the GALINAUTE II cruise (Nautile dives on the Galicia Bank, Spain). *C.R. Académie des Sciences*, **321**, II a, 1171–1178.

BOUDIER, F., JACKSON, M. & NICOLAS, A. 1984. Structural study of the Balmuccia massif (Western Alps): a transition from mantle to lower crust. *Geologie en Mijnbouw*, **63**, 179–188.

BOULLIER, A. M. & GUEGUEN, Y. 1975. SP-Mylonites: origin of some mylonites by superplastic flow. *Contributions to Mineralogy and Petrology*, **50**, 93–104.

BRODIE, K. H. 1980. Variations in mineral chemistry across a shear zone in phlogopite peridotite. *Journal of Structural Geology*, **2**, 265–272.

BRODIE, K. H. & RUTTER, E. H. 1985. On the Relationship between Deformation and Metamorphism with Special Reference to the Behavior of Basic Rocks. *In*: THOMPSON, A. B. & RUBIE, D. (eds) *Kinematics, Textures and Deformation*. Advances in Physical Geochemistry, Springer Verlag, 138–179.

BRODIE, K. H. & RUTTER, E. H. 1987*a*. Deep crustal extensional faulting in the Ivrea Zone of Northern Italy. *Tectonophysics*, **140**, 183–212.

BRODIE, K. H. & RUTTER, E. H. 1987b. The role of transiently fine-grained reaction products in syntectonic metamorphism: natural and experimental examples. *Canadian Journal of Earth Sciences*, **24**, 556–564.

BRUN, J.-P. & BESLIER, M. O. 1996. Mantle exhumation of passive margins. *Earth and Planetary Science Letters*, **142**, 161–173.

BUCHER, K. & FREY, M. 1994. *Petrogenesis of Metamorphic Rocks*. Springer-Verlag, Berlin.

CALLOT, J.-P., GRIGNE, C., GEOFFREY, L. & BRUN, J.-P. 2001. Development of volcanic passive margins: Two dimensional laboratory models. *Tectonics*, **20**, 148–159.

CHAPMAN, D. S. 1986. Thermal gradients in the continental crust. *In*: DAWSON, J. B., CARSWELL, D. A., HALL, J. & WEDEPOHL, K. H. (eds) *The nature of the lower continental crust*. Geological Society, London, Special Publications, **24**, 51–62.

CHEN, W.-P. & MOLNAR, P. 1983. Focal depths of intracontinental earthquakes and their correlations with heat flow and tectonic age. *Seismological Research Lettters*, **59**, 263–272.

DE BRESSER, J. H. P., TER HEEGE, J. H. & SPIERS, C. J. 2001. Grain size reduction by dynamic recrystallization: can it result in major rheological weakening? *International Journal of Earth Sciences*, **90**, 28–45.

DIXON, J. & WILLIAMS, G. 1983. Reaction softening in mylonites from the Arnaboll thrust, Sutherland. *Scottish Journal of Geology*, **19**, 157–168.

DRURY, M. R., VISSERS, R. L. M., HOOGERDUIJN STRATING, E. H. & VAN DER WAL, D. 1991. Shear localisation in upper mantle peridotites. *Pure and Applied Geophysics*, **137**, 439–460.

EVANS, J. P. 1991. Textures, deformation mechanisms and the role of fluid in the cataclastic deformation of granitic rocks. *In*: KNIPE, R. J. & RUTTER, E. H. (eds) *Deformation Mechanisms, Rheology, and Tectonics*. Geological Society, London, Special Publications, **54**, 29–41.

FAVRE, P. & STAMPFLI, G. M. 1992. From rifting to passive margin: examples of the Red Sea, Central Atlantic and Alpine Tethys. *Tectonophysics*, **215**, 69–97.

FITZGERALD, J. D. & STÜNITZ, H. 1993. Deformation of granitoids at low metamorphic grade. I: reactions and grain size reduction. *Tectonophysics*, **221**, 269–297.

FROITZHEIM, N. & MANATSCHAL, G. 1996. Kinematics of Jurassic rifting, mantle exhumation, and passive-margin formation in the Austroalpine and Penninic nappes (eastern Switzerland). *Geological Society of America Bulletin*, **108**, 1120–1133.

FURUSHO, M. & KANAGAWA, K. 1999. Transformation-induced strain localization in a lherzolite mylonite from the Hidaka metamorphic belt of central Hokkaido, Japan. *Tectonophysics*, **313**, 411–432.

GANDHI, C. & ASHBY, M. F. 1979. Fracture-mechanisms maps for materials which cleave: F.C.C., B.C.C. and H.C.P. metals and ceramics. Overview No. 5. *Acta Metallurgica*, **27**, 1565–1602.

GARUTI, G. & FRIOLO, R. 1978/79. Textural features and olivine fabrics of peridotites from the Ivrea–Verbano Zone (Italian western Alps). *Memorie di Scienze Geologiche*, **33**, 111–125.

GASPARIK, T. 1987. Orthopyroxene thermobarometry in simple and complex systems. *Contributions to Mineralogy and Petrology*, **96**, 357–370.

GROCOTT, J. & WATTERSON, J. 1980. Strain profile of a boundary within a large ductile shear zone. *Journal of Structural Geology*, **2**, 111–117.

HANDY, M. R. 1987. The structure, age, and kinematics of the Pogallo fault zone, Southern Alps, northwestern Italy. *Eclogae geologicae Helvetiae*, **80**, 593–632.

HANDY, M. R. 1989. Deformation regimes and the rheological evolution of fault zones in the lithosphere: the effects of pressure, temperature, grain size, and time. *Tectonophysics*, **163**, 119–152.

HANDY, M. R. 1994. The energetics of steady state heterogeneous shear in mylonitic rock, *Materials Science and Engineering*, **A175**, 261—272.

HANDY, M. R. & ZINGG, A. 1991. The tectonic and rheologic evolution of the Ivrea Crustal Cross Section (Southern Alps of northwestern Italy and southern Switzerland). *Geological Society of America Bulletin*, **103**, 236–253.

HANDY, M. R., FRANZ, L., HELLER, F., JANOTT, B. & ZURBRIGGEN, R. 1999. Multistage accretion and exhumation of continental (Ivrea crustal section, Italy and Switzerland). *Tectonics*, **18**, 1154–1177.

HOBBS, B. E., MUHLHAUS, H.-B. & ORD, A. 1990. Instability, softening and localization of deformation. *In*: KNIPE, R. J. & RUTTER, E. H. (eds) *Deformation Mechanisms, Rheology and Tectonics*. Geological Society, London, Special Publications, **45**, 143–166.

JAROSLOW, G. E., HIRTH, G. & DICK, H. J. B. 1996. Abyssal peridotite mylonites: implications for grain-size sensitive flow and strain localization in the oceanic lithosphere. *Tectonophysics*, **256**, 17–37.

JIN, D., KARATO, S.-I. & OBATA, M. 1998. Mechanisms of shear localization in the continental lithosphere: inference from the deformation microstructures of peridotites from the Ivrea zone, northwestern Italy. *Journal of Structural Geology*, **20**, 195–209.

KARSONS, J. A. 1991. Accommodation zones and transfer faults: integral components of Mid-Atlantic Ridge extensional systems. *In*: PETERS, T., NICOLAS, A. & COLEMAN, R. J. (eds) *Ophiolite Genesis and Evolution of Oceanic Lithosphere*. Ministry of Petroleum and Minerals, Sultanate of Oman, 21–37.

KEEN, C. E., MCLEAN, B. C. & KAY, W. A. 1991. A deep seismic reflection profile across the Nova Scotia continental margin offshore eastern Canada. *Canadian Journal of Earth Sciiences*, **28**, 1112–1120.

KIRBY, S. H. 1985. Rock mechanics observations pertinent to the rheology of the continental lithosphere and the localization of strain along shear zones. *Tectonophysics*, **118**, 1–27.

KRONENBERG, A. K., SEGALL, P. & WOLF, G. H. 1990. Hydrolytic Weakening and Penetrative Deformation Within a Natural Shear Zone. *In*: DUBA, A. G., DURHAM, W. B., HANDIN, J. W. & WANG, H. F. (eds) *The brittle-ductile transition in rocks, the Heard volume*, AGU Geophysical Monograph, **56**, 21–36.

KRUHL, J. H. & VOLL, G. 1978/79. Deformation and Metamorphism of the Western Finero Complex. *Memorie di Scienze Geologiche*, **33**, 95–109.

KRUSE, R. & STÜNITZ, H. 1999. Deformation mechanisms and phase distribution in mafic, high-temperature mylonites from the Jotun Nappe, southern Norway. *Tectonophysics*, **303**, 223–250.

LEMOINE, M., TRICART, P. & BOILLOT, G. 1987. Ultramafic and gabbroic ocean floor of the Ligurian Tethys (Alps, Corsica, Apennines): in search of a genetic model. *Geology*, **15**, 622–625.

LIN, A. 1997. Ductile deformation of biotite in foliated cataclasite, Iida-Matsukawa fault, central Japan. *Journal of Asian Earth Sciences*, **15**, 407–411.

LISTER, G. S., ETHERIDGE, M. A. & SYMONDS, P. A. 1991. Detachment models for the formation of passive continental margins. *Tectonics*, **10**, 1038–1064.

MAGGI, A., JACKSON, J. A., MCKENZIE, D. & PRIESTLEY, K. 2000. Earthquake focal depths, effective elastic thickness, and the strength of the continental lithosphere. *Geology*, **28**, 495–498.

MCGEARY, S. & WARNER, M. 1985. Seismic profiling of the lower continental lithosphere. *Nature*, **317**, 795–797.

MCKENZIE, D., NIMMO, F. & JACKSON, J. A. 2000. Characteristics and consequences of flow in the lower crust. *Journal of Geophysical Research*, **105**, 11029–11046.

MITRA, G. 1978. Ductile deformation zones and mylonites: the mechanical processes involved in the deformation of crystalline basement rocks. *American Journal of Science*, **278**, 1057–1084.

MÜNTENER, O. & HERMANN, J. 2001. The role of lower crust and continental upper mantle during formation of non-volcanic passive margins: evidence from the Alps. *In*: WILSON, R. C. L., WHITMARSH, R. B., TAYLOR, B. & FROITZHEIM, N. (eds) *Non-volcanic rifting of continental margins: a comparison of evidence from land and sea*. Geological Society, London, Special Publications, **187**, 267–288.

NEWMAN, J., LAMB, W. M., DRURY, M. R. & VISSERS, R. L. M. 1999. Deformation processes in a peridotite shear zone: reaction-softening by an H_2O-deficient, continuous net transfer reaction. *In*: SCHMID, S. M., HEILBRONNER, R. & STÜNITZ, H. (eds) *Deformation Mechanisms in Nature and Experiment*. *Tectonophysics*, **303**, 193–222.

NIIDA, K. & GREEN, D. H. 1999. Stabilty and chemical composition of pargasitic amphibole in MORB pyrolite under upper mantle conditions. *Contributions to Mineralogy and Petrology*, **135**, 18–40.

OBATA, M. 1976. The solubility of Al_2O_3 in orthopyroxenes in spinel and plagioclase peridotites and spinel pyroxenite. *American Mineralogist*, **61**, 804–816.

OBATA, M. & KARATO, S. 1995. The solubility of Al_2O_3 ultramafic pseudotachylite from the Balmuccia peridotite, Ivrea–Verbano zone, northern Italy. *Tectonophysics*, **242**, 313–328.

PATERSON, M. S. 1987. Problems in the extrapolation of laboratory rheological data. *Tectonophysics*, **133**, 33–43.

PATERSON, M. S. & OLGAARD, D. L. 2000. Rock deformation to large strains in torsion. *Journal of Structural Geology*, **22**, 1341–1358.

POIRIER, J. P. & NICOLAS, A. 1975. Deformation-induced recrystallization due to progressive misorientation of subgrains, with special reference to mantle peridotites. *Journal of Geology*, **83**, 707–720.

QUICK, J. E., SINIGOI, S. & MAYER, A. 1994. Emplacement dynamics of a large mafic intrusion in the lower crust, Ivrea–Verbano, northern Italy. *Journal of Geophysical Research*, **99**, 21559–21573.

RALEIGH, C. B. & PATERSON, M. S. 1965. Experimental deformation of serpentinite and its tectonic implications. *Journal of Geophysical Research*, **70**, 3965–3985.

RANALLI, G. & MURPHY, D. C. 1987. Rheological stratification of the lithosphere. *Tectonophysics*, **132**, 281–296.

RESTON, T. 1987. Spatial interference, reflection character and the structure of the lower crust under extension – Results from 2-D seismic modelling. *Annales Geophysicae*, **5B**, 339–348.

RESTON, T. 1990. Shear in the lower crust during extension: not so pure and simple. *Tectonophysics*, **173**, 175–183.

RIVALENTI, G., GARUTI, G. & ROSSI, A. 1975. The origin of the Ivrea–Verbano basic formation (Western Italian Alps). *Bolletino Societa Geologica Italiana*, **94**, 1149–1186.

RIVALENTI, G., GARUTI, G., ROSSI, A., SIENA, F. & SINIGOI, S. 1981. Existence of different peridotite types and of a layered igneous complex in the Ivrea Zone of the Western Alps. *Journal of Petrology*, **22**, 127–153.

RIVALENTI, G., ROSSI, A., SIENA, F. & SINIGOI, S. 1984. The Layered Series of the Ivrea- Verbano Igneous Complex, Western Alps, Italy. *Tschermaks Mineralogische und Petrographische Mitteilungen*, **33**, 77–99.

RUTTER, E. H. & BRODIE, K. H. 1988. The role of tectonic grainsize reduction in the rheological stratification of the lithosphere. *Geologische Rundschau*, **77**, 295–308.

SAVOSTIN, L. A., SIBUET, J.-C., ZONENSHAIN, L. P., LE PICHON, X. & ROULET, M.-J. 1986. Kinematic evolution of the Tethys belt from the Atlantic Ocean to the Pamirs since the Triassic. *Tectonophysics*, **123**, 1–35.

SCHMID, S. M. 1993. Ivrea Zone and Adjacent Southern Alpine Basement. *In*: VON RAUMER, J. F. & NEUBAUER, F. (eds) *Pre-Mesozoic Geology in the Alps*. Springer Verlag, Berlin, 567–584.

SCHMID, S. M. & KISSLING, E. 2000. The arc of the western Alps in the light of geophysical data on deep crustal structure. *Tectonics*, **19**, 62–85.

SCHMID, S. M., AEBLI, H. R., HELLER, F. & ZINGG, A. 1989. The role of the Periadriatic Line in the tectonic evolution of the Alps. *In*: COWARD, M. P., DIETRICH, D. & PARK, R. (eds) *Alpine Tectonics*. Geological Society, London, Special Publications, **45**, 153–171.

SCHMID, S. M., PANOZZO, R. & BAUER, S. 1987. Simple shear experiments on calcite rocks: rheology and microfabrics. *Journal of Structural Geology*, **9**, 747–778.

SEGALL, P. & POLLARD, D. D. 1983. Nucleation and grwoth of strike-slip faults in granite. *Journal of Geophysical Research*, **88**, 555–568.

SEGALL, P. & SIMPSON, C. 1986. Nucleation of ductile shear zones on dilatant fractures. *Geology*, **14**, 56–59.

SHERVAIS, J. W. 1979. Thermal emplacement model for the Alpine Lherzolite massif at Balmuccia, Italy. *Journal of Petrology*, **20**, 795–820.

SINIGOI, S., QUICK, J., CLEMENS-KNOTT, D., MAYER, A. & DEMARCHI, G. 1994. Chemical evolution of a large mafic intrusion in the lower crust, Ivrea–Verbano Zone. *Journal of Geophysical Research*, **99**, 21575–21590.

SKROTZKI, W., WEDEL, A., WEBER, K. & MÜLLER, W. F. 1990. Microstructure and texture in lherzolites of the Balmuccia massif and their significance regarding the thermomechanical history. *Tectonophysics*, **179**, 227–251.

STAMPFLI, G. M. & MARTHALER, M. 1990. Divergent and convergent margins in the North-Western Alps confrontation to actualistic models. *Geodinamica Acta*, **3**, 159–184.

STECK, A. & TIÈCHE, J.-C. 1976. Carte geologique de l'antiforme peridotique de Finero avec des observations sur les phases de deformation et de recristallisation. *Bulletin de Minéralogie et Pétrographie de Suisse*, **56**, 501–512.

STÜNITZ, H. 1993. Transition from fracturing to viscous flow in a naturally deformed metagabbro. *In*: BOLAND, J. N. & FITZGERALD, J. D. (eds) *Defects and Processes in the Solid State: Geoscience Applications, the McLaren Volume*, Elsevier, Amsterdam, 121–150.

STÜNITZ, H. & TULLIS, J. 2001. Weakening and strain localization produced by syndeformational reaction of plagioclase. *International Journal of Earth Sciences*, **90**, 136–148.

STUNITZ, H., TULLIS, J. & YUND, R. 1999. The relation between deformation and reaction for experimentally deformed olivine + plagioclase. *EOS Transactions*, **80**, 1021.

TECHMER, K. S., AHRENDT, H. & WEBER, K. 1993. The development of pseudotachylite in the Ivrea–Verbano zone of the north Italian Alps. *Tectonophysics*, **204**, 307–322.

TROMMSDORFF, V. 1983. Metamorphose magensiumreicher Gesteine: Kritischer Vergleich von Natur, Experiment und thermodynamischer. *Datenbasis. Fortschr. Mineral.*, **61**, 283–308.

TROMMSDORFF, V. & EVANS, B. W. 1974. Alpine metamorphism of peridotitic rocks. *Schweizerische Mineralogische und Petrographische Mitteilungen*, **54**, 333–352.

TROMMSDORFF, V., PICCARDO, G. B. & MONTRASIO, A. 1993. From magmatism through metamorphism to sea floor emplacement of subcontinental Adria lithosphere during pre-Alpine rifting (Malenco, Italy). *Schweizerische Mineralogische und Petrographische Mitteilungen*, **73**, 191–203.

TULLIS, J. & YUND, R. A. 1985. Dynamic recrystallization of feldspar: a mechanism for ductile shear zone formation. *Geology*, **13**, 238–241.

TULLIS, J., DELL'ANGELLO, L. & YUND, R. A. 1990. Ductile shear zones from brittle precursors in feldspathic rocks: The role of dynamic recrystallization. *In*: DUBA, A. G., DURHAM, W. B., HANDIN, J. W. & WANG, H. F. (eds) *The Brittle-ductile Transition in Rocks, the Heard Volume*. Geophysical Monograph, **56**, 67–82.

TUSCHOLKE, B. E. & LIN, J. 1994. A geological model for the structure of ridge segments in slow-spreading oceanic crust. *Journal of Geophysical Research*, **99**, 11937–11958.

VAN DER WAL, D., CHOPRA, P. N., DRURY, M. R. & FITZGERALD, J. D. 1993. Relationships between dynamically recrystallized grain size and stress in experimentally deformed olivine rocks. *Geophysical Research Letters*, **20**, 1479–1482.

VAVRA, G., SCHMID, R. & GEBAUER, D. 1999. Internal morphology, habit and U-Th-Pb microanalysis of amphibolite-to-granulite facies zircons: geochronology of the Ivrea Zone (Southern Alps). *Contributions to Mineralogy and Petrology*, **134**, 380–404.

VISSERS, R. L. M., DRURY, M. R., HOOGERDUIJN STRATING, E. H., SPIERS, E. H. & VAN DER WAL, D. 1995. Mantle shear zones and their effect on lithosphere strength during continental break-up. *Tectonophysics*, **249**, 155–171.

VISSERS, R. L. M., DRURY, M. R., HOOGERDUIJN STRATING, E. H. & VAN DER WAL, D. 1991. Shear zones in the upper mantle: A case study in an Alpine lherzolite massif. *Geology*, **19**, 990–993.

VISSERS, R. L. M., DRURY, M. R., NEWMAN, J. & FLIERVOET, T. F. 1997. Mylonitic deformation in upper mantle peridotites of the North Pyrenean Zone (France): implications of strength and strain localization in the lithosphere. *Tectonophysics*, **279**, 303–325.

WALLACE, M. E. & GREEN, D. H. 1991. The effect of bulk rock composition on the stability of amphibole in the upper mantle: implications for the solidus positions and mantle metasomatism. *Mineralogy and Petrology*, **44**, 1–19.

WALTER, M. J. & PRESNALL, D. C. 1994. Melting behaviour of simplified lherzolite in the system CaO-MgO-Al_2O_3-SiO_2-Na_2O_3 from 7 to 35 kb. *Journal of Petrology*, **35**, 329–359.

WEERTMAN, J. 1970. The creep strength of the Earth's mantle. *Reviews of Geophysics and Space Physics*, **8**, 145–168.

WERNICKE, B. 1985. Uniform-sense normal simple shear of the continental lithosphere. *Canadian Journal of Earth Sciences*, **22**, 108–125.

WHITE, S. H. & KNIPE, R. J. 1978. Transformation- and reaction-enhanced ductility in rocks. *Journal of the Geological Society, London*, **135**, 513–516.

WIBBERLEY, C. 1999. Are feldspar-to-mica reactions necessarily reaction-softening processes? *Journal of Structural Geology*, **21**, 1219–1227.

WILSON, C. J. L. & BELL, I. A. 1979. Deformation of biotite and muscovite: optical microstructure. *Tectonophysics*, **58**, 179–200.

WINTSCH, R. P., CHRISTOFFERSEN, R. & KRONENBERG, A. K. 1995. Fluid-rock reaction weakening of fault zones. *Journal of Geophysical Research*, **100**, 13021–13032.

ZEUCH, D. H. 1982. Ductile faulting, dynamic recrystallization and grain-size sensitive flow of olivine. *Tectonophysics*, **83**, 293–308.

ZEUCH, D. H. 1983. On the inter-relationship between grain-size sensitive creep and dynamic recrystallization of olivine. *Tectonophysics*, **93**, 151–168.

ZINGG, A., HANDY, M. R., HUNZIKER, J. C. & SCHMID, S. M. 1990. Tectonometamorphic history of the Ivrea Zone and its relation to the crustal evolution of the Southern Alps. *Tectonophysics*, **182**, 169–192.